

Symmetry-Adapted No-Core Shell-Model Calculations for Probing the Structure of Atomic Nuclei

J. P. Draayer^a, K. D. Launey^a, T. Dytrych^{a,b}, R. B. Baker^a,
A. C. Dreyfuss^a, D. Kekejian^a and G. H. Sargsyan^a

^a*Department of Physics and Astronomy, Louisiana State University, Baton Rouge, LA 70803-4001, USA*

^b*Nuclear Physics Institute, 250 68 Řež, Czech Republic*

Abstract

The use of symmetries to unmask simplicity within complexity in atomic nuclei is examined within its historical context and the evolving *ab initio* no-core shell model (NCSM) approaches that typically rely heavily on high-performance computing and applied math methods. Some examples — old and new — that demonstrate the important role symmetries plays in this evolution, are noted. Further, an extension of the symmetry adapted no-core shell model (SA-NCSM), one that incorporates deformation from the onset, is proffered as a potential path forward for further reducing the combinatorial growth of model-space sizes that are required to track collective phenomena in a non-deformed theory. This feature suggests a means for extending *ab initio* methods to even heavier nuclei.

Keywords: *Ab initio theory; no-core shell model (NCSM); symmetry-adapted NCSM; symplectic model; deformed configurations; many-particle Nilsson model*

1 Introduction

This contribution is organized into five sections: 1) A short ‘Introduction’ (i. e., this paragraph) that lays out the structure of this report, 2) A brief ‘Historical overview’ of efforts — old and new — focused on expanding shell-model spaces to reproduce collective and clustering features (principal co-author A. Dreyfuss), 3) Some recent ‘Exemplary results’ which show that special symmetries can be used to tame the combinatorial growth of NCSM model spaces while extending their reach, and to reproduce observed enhanced $B(E2)$ transition strengths without the use of effective charges (principle co-authors R. Baker and G. Sargsyan), 4) How ‘Canonical transformations’ from non-deformed to deformed many-particle configurations that preserve these special symmetries can be used to gain further reductions in model space sizes — essentially an interacting many-particle Nilsson model (principal co-author D. Kekejian), and 5) A ‘Conclusion’ that looks beyond the current landscape to more novel

Proceedings of the International Conference ‘Nuclear Theory in the Supercomputing Era — 2018’ (NTSE-2018), Daejeon, South Korea, October 29 – November 2, 2018, eds. A. M. Shirokov and A. I. Mazur. Pacific National University, Khabarovsk, Russia, 2019, p. 279.

<http://www.ntse.khb.ru/files/uploads/2018/proceedings/Draayer.pdf>.

notions that just as special symmetries carry one from the NCSM to its symmetry-adapted extension, SA-NCSM, should enable use of *ab initio* methods in studies of heavier nuclei.

2 Historical overview

The independent-particle model of Mayer and Jensen [1, 2], with its reproduction of the ‘magic’ numbers of nuclei, can arguably be called the first microscopic theory of nuclear structure. Its success inspired the development of various follow-on models of increasing levels of sophistication across the second half of the last century. However, testing these theories against experimental data was limited by meager computational resources, up until about the last decade or so of that period. The advent of truly high-performance computational resources in the 90s enabled the development and testing of so-called no-core shell model (NCSM) concepts [3, 4] (see, e. g., Refs. [5–7]), which to date have been used to describe the structure of low-lying states of *s*- and *p*-shell nuclei, starting from *ab initio* principles.

The NCSM preserves exact symmetries like time reversal invariance, parity conservation, and translational invariance within an overarching many-particle framework that respects particle number conservation and statistics; that is, the NCSM is a fully microscopic many-fermion theory of nuclear structure that uses realistic interactions between and among nucleons that reside in properly anti-symmetrized bases states built from single-particle states of the three-dimensional harmonic oscillator (3D-HO), where the energy scale of the latter is set by the $\hbar\Omega$ parameter of the oscillator.

Within the NCSM framework, the complete model space is organized into the horizontal slices of the HO, each separated in energy from its neighbors by $\hbar\Omega$, with interactions among particles within a slice as well as between particles in neighboring slices accounted for, up to some N_{\max} cutoff which is the maximum total number of oscillator quanta above the lowest HO configuration for a given nucleus, thereby reducing the infinite model space to a truncated subspace of the full space, one capped by the $N_{\max}\hbar\Omega$ cutoff limit imposed on the theory. In the $N_{\max}\hbar\Omega \rightarrow$ infinity limit, the theory encompasses the entire shell-model space.

While the independent-particle model approach was being developed, there was a complementary push towards models that describes the observed strongly collective features found in nuclei. Some notable early models that reproduce collective features are the Bohr–Mottelson Model (BMM) for collective nuclear motion [8], the Geometrical Collective Model (GCM) of the Greiner school [9, 10], and of particular relevance to this report, the Elliott SU(3) Model [11, 12]. Specifically, the Elliott model captures the importance of the SU(3) symmetry in describing — from a microscopic perspective — the deformed structures in light to intermediate-mass nuclei. A similar approach using pseudo-spin symmetry and its pseudo-SU(3) complement has been used to describe deformation in the upper *pf* and lower *sdg* shells, and in particular, in strongly deformed nuclei of the rare-earth and actinide regions [13], as well as in many other studies (e. g., see Ref. [14]). The collective symplectic model developed by Rowe and Rosensteel [15, 16], with the $\text{Sp}(3, \mathbb{R})$ underpinning symmetry, intersects with these collective approaches. In one limit, the symplectic model can be shown to be a microscopic realization of the Bohr–Mottelson theory, and, in another, a multi-shell generalization of the Elliott model, with SU(3) being a subgroup of $\text{Sp}(3, \mathbb{R})$.

First-principles SA-NCSM — Building on the foundations of particle-driven models, such as the NCSM, and the use of symmetries to reproduce collectivity, as in the collective symplectic model, the *ab initio* symmetry-adapted no-core shell model (SA-NCSM) is a no-core shell model with a symmetry-adapted basis that is either $SU(3)$ -coupled or $Sp(3, \mathbb{R})$ -coupled. In the $SU(3)$ -coupled realization, basis states are organized with respect to the physically relevant, deformation-related $SU(3)_{(\lambda\mu)} \supset^{\kappa} SO(3)_L$ subgroup chains. In a given complete N_{\max} model space, results for the SA-NCSM and NCSM coincide exactly, for the same interaction. The use of symmetries to guide SA-NCSM model space selection allows for the consideration of only the most physically-relevant subspace of a complete N_{\max} model space. The SA-NCSM uses a very general intrinsic non-relativistic Hamiltonian

$$H = T_{\text{rel}} + V_{\text{NN}} + V_{3\text{N}} + \dots + V_{\text{Coul}}, \quad (1)$$

where T_{rel} is the relative kinetic energy, and the nucleon-nucleon, V_{NN} , and possibly 3-nucleon, $V_{3\text{N}}$, interactions are included along with the Coulomb interaction, V_{Coul} , between the protons.

First-principles studies of p -shell nuclei computed in the *ab initio* SA-NCSM show the emergence of a simple pattern that favors large deformation and low spin (Fig. 1). For example, the SA-NCSM wave function for the 1^+ ground state of ${}^6\text{Li}$ computed in an $N_{\max} = 10$ model space with the bare JISP16 nucleon-nucleon (NN) interaction is dominated by the deformed $0\hbar\Omega$ (2 0) irreducible representation (irrep) and its symplectic excitations (e. g., $2\hbar\Omega$ (4 0), $4\hbar\Omega$ (6 0), etc.). This pattern is seen in studies of other p -shell nuclei, including ${}^6\text{He}$, ${}^8\text{Be}$, and ${}^{12}\text{C}$, using various realistic NN interactions, including chiral interactions. This universality of this emergent feature underlines the importance of the $SU(3)$ and $Sp(3, \mathbb{R})$ symmetries in describing nuclear structure.

No-core Symplectic Shell Model (NCSpM) — The symplectic $Sp(3, \mathbb{R})$ symmetry applied in a microscopic framework is directly related to the particle position and momentum coordinates, and naturally describes rotations and vibrations of an equilibrium deformation [17, 18]. By exploiting this emergent symmetry, the microscopic no-core symplectic shell model (NCSpM) [19] makes use of a schematic interaction to approach model spaces beyond what is currently within reach of *ab initio* theories. The NCSpM is a fully microscopic no-core shell model based on the physically relevant symplectic $Sp(3, \mathbb{R})$ group [15, 16] and its $SU(3)$ subgroup [11, 12, 20]. In the same complete N_{\max} model space and using the same interaction, the NCSM and NCSpM results are identical. In analogy to the NCSM horizontal slices of the complete model space, the NCSpM organizes the complete space into a series of vertical ‘cones’ within the HO well, which are irreps of $Sp(3, \mathbb{R})$, included up to some N_{\max} . Each of these irreps described a single equilibrium deformation and its rotations and vibrations. By including only a few of these cones, the model space is greatly reduced, which allows extension to higher N_{\max} model spaces beyond the current NCSM limits, giving access to the spaces needed to probe clustering in nuclei.

The microscopic NCSpM uses a many-body Hamiltonian that includes a collective piece that enters through the quadrupole-quadrupole interaction, as described in Ref. [19, 21]:

$$H = T_{\text{rel}} + V_{\text{NN}} + V_{\text{mN}}^{\text{eff}} + \dots + V_{\text{Coul}}. \quad (2)$$

The V_{NN} is taken to be the bare JISP16 nucleon-nucleon interaction, which is turned

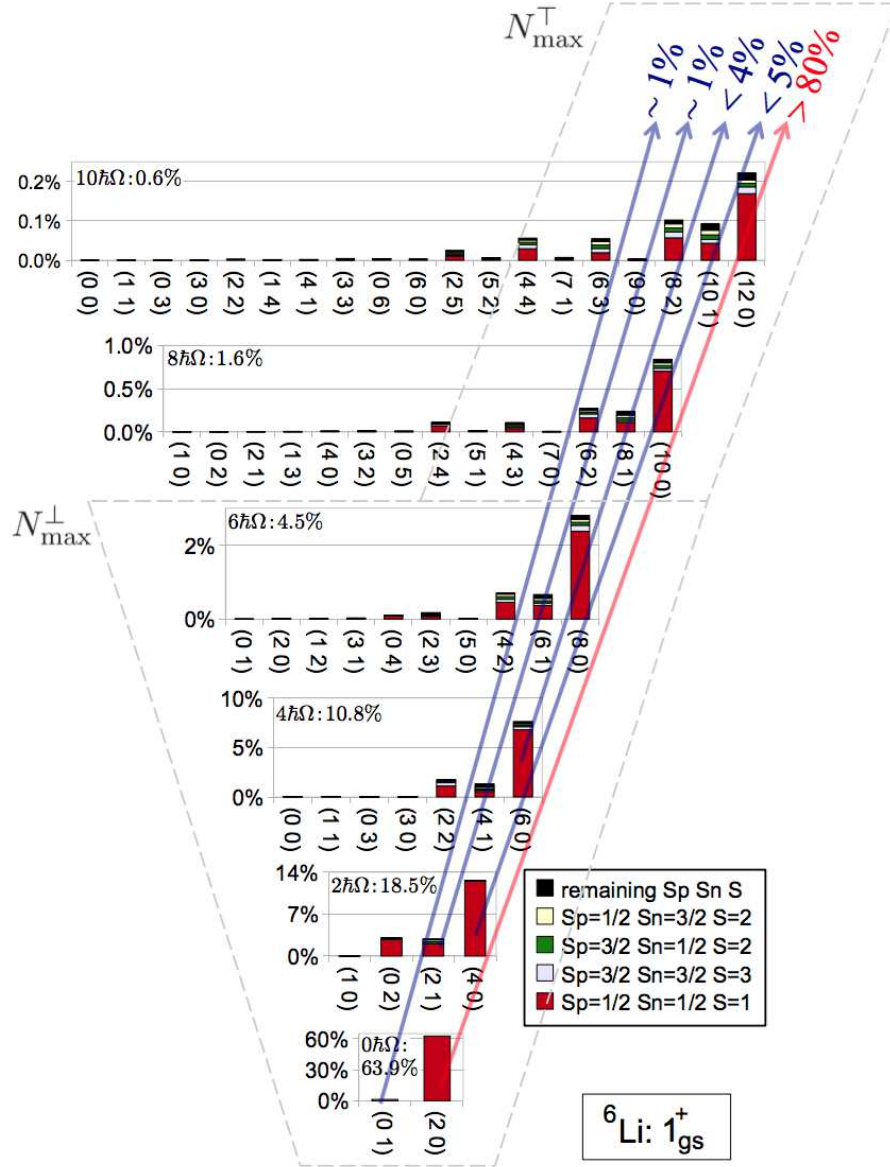


Figure 1: Probability distributions for proton, neutron, and total intrinsic spin components ($S_p S_n S$) across the Pauli-allowed deformation-related ($\lambda\mu$) values for the 1^+ ground state of ${}^6\text{Li}$, calculated in 12 HO shells with the JISP16 bare interaction ($\hbar\Omega = 20$ MeV). The most deformed configurations ($\lambda\mu$) are at the right of each HO shell subspace, where the strengths are concentrated indicating the dominance of collectivity. A symmetry-guided model-space selection takes advantage of this emergent property by including the full space up through N_{max}^\perp , but then selecting a subset of configurations with high deformation and low spin up through N_{max}^\top . A model space constructed in this way is labeled $\langle N_{\text{max}}^\perp \rangle N_{\text{max}}^\top$. The projection onto symplectic vertical slices (with probability $\geq 1\%$) is schematically illustrated by arrows and clearly reveals the preponderance of a single symplectic irrep. Adapted from Ref. [17].

on only among bandheads of symplectic irreps, introducing horizontal mixing of all the states (up through the N_{\max} cutoff) within the symplectic vertical slices. The effective many-nucleon interaction is taken to be $V_{\text{mN}}^{\text{eff}} = \sum_{i=1}^A \frac{m\Omega^2 \mathbf{r}_i^2}{2} + \frac{\chi}{2} \frac{(e^{-\gamma(Q \cdot Q)} - 1)}{\gamma}$. The symplectic $\text{Sp}(3, \mathbb{R})$ symmetry is preserved by the HO potential and T_{rel} , and the important quadrupole-quadrupole interaction $\frac{1}{2} Q \cdot Q = \frac{1}{2} \sum_i q_i \cdot (\sum_j q_j)$, which introduces the interaction of each particle with the total quadrupole moment of the system.¹ The value of χ is fixed using self-consistent arguments [22] by the estimate used in an $\text{Sp}(3, \mathbb{R})$ -based study of cluster-like states of ^{16}O [23], and the strength of the HO potential is fixed using the empirical estimate $\hbar\Omega \approx 41/A^{1/3}$. The only adjustable parameter in the model is γ . The H_γ potential term introduces many-body interactions hierarchically, controlled by $\gamma < 1$, such that higher-order terms in the exponential of $Q \cdot Q$ become negligible. For example, we find that for the ^{12}C ground state, all terms in the expansion beyond $(Q \cdot Q)^2$ contribute negligibly to the wave function. However, the ^{12}C Hoyle state band, requires the inclusion of terms up through $(Q \cdot Q)^4$ (or the third order in γ) [19].

The energy spectrum for ^{12}C , computed in the NCSpm with $N_{\max} = 20$ and $\hbar\Omega = 18$ MeV down-selected to only 5 symplectic irreps, agrees remarkably well with experiment (Fig. 2). We find that the lowest 0^+ , 2^+ , and 4^+ states of the two $0p-0h$ irreps [$0p-0h$ (4 0) and $0p-0h$ (1 2)] reproduce the ground state rotational band. The lowest 0^+ state of the $4p-4h$ (12 0) irrep coincides with the experimental Hoyle state, and the lowest 0^+ state of the $2p-2h$ (6 2) irrep coincides with the third 0^+ in ^{12}C . The low-lying 3^- state is reproduced using the $1p-1h$ (3 3) irrep. The one-body (matter) densities shown in Fig. 2 (right) indicate a donut-like shape for the ^{12}C ground state, while the 0_2^+ state shows peaks in the probability density aligned along the z -axis, indicating overlapping clusters spatially extended along this axis. While a smaller N_{\max} model space is sufficient for convergence of the ground state rotational band, the wave function for the 0_2^+ state of ^{12}C has significant contributions from highly deformed configurations [e. g., (12 0), (14 0), (16 0), etc.] and requires a much larger N_{\max} model space in order for the collectivity of the state to fully develop and for the energy to reach convergence.

In addition to the energy spectrum, the NCSpm reproduces observables such as $B(E2)$ transition strengths (Fig. 2), matter rms radii, and electric quadrupole moments, and has been used to investigate the nature of the giant monopole and quadrupole resonances in selected light- and intermediate-mass nuclei [25]. This model has also been applied to studies of other nuclei, including ^8Be , as well as various sd -shell nuclei without the need to adjust the γ strength parameter [26, 27]. Its ability to reproduce energy spectra as well as collective features in various nuclei indicates that the NCSpm captures important components of the underlying nuclear physics.

3 Exemplary results

Ab initio SA-NCSM calculations have now been extended into and beyond the intermediate mass region as shown in Fig. 3, including odd- A nuclei and their negative parity states (e. g., ^{19}Ne in 12 HO major shells [28]) and nuclei near the dripline (e. g.,

¹Note, the average value of $Q \cdot Q$ within an oscillator shell introduces a major renormalization of the HO shell structure, so, as is normally done, this average is removed; that is, $Q \cdot Q \rightarrow (Q \cdot Q - \langle Q \cdot Q \rangle)$, where the average $\langle Q \cdot Q \rangle$ has a simple universal operator form that applies to a HO shell.

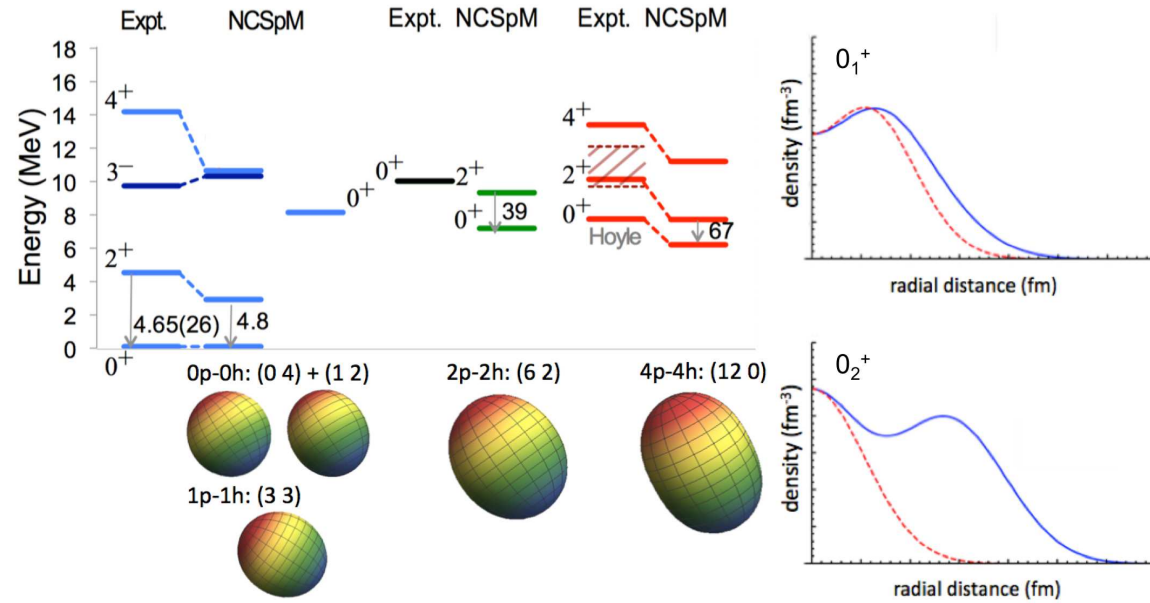


Figure 2: **Left:** Energy spectrum for ^{12}C calculated using the NCSpM with the schematic interaction (2) and the JISP16 NN interaction as the V_{NN}^{SB} symmetry-breaking term, and using 5 $\text{Sp}(3, \mathbb{R})$ irreps (the average deformation of each is depicted at bottom) extended to $N_{\text{max}} = 20$ ($\hbar\Omega = 18$ MeV), and compared to experiment. $B(E2)$ transition strengths are in W.u. **Right:** Densities, shown along the x -axis (dashed) and z -axis (solid) of the intrinsic frame for the ground state and the 0_2^+ state. Components of the wave function with probability $> 3\%$ are included, comprising 95% of the ground state wave function, and 91% of the wave function for the 0_2^+ state. The figures are adapted from Refs. [21, 24].

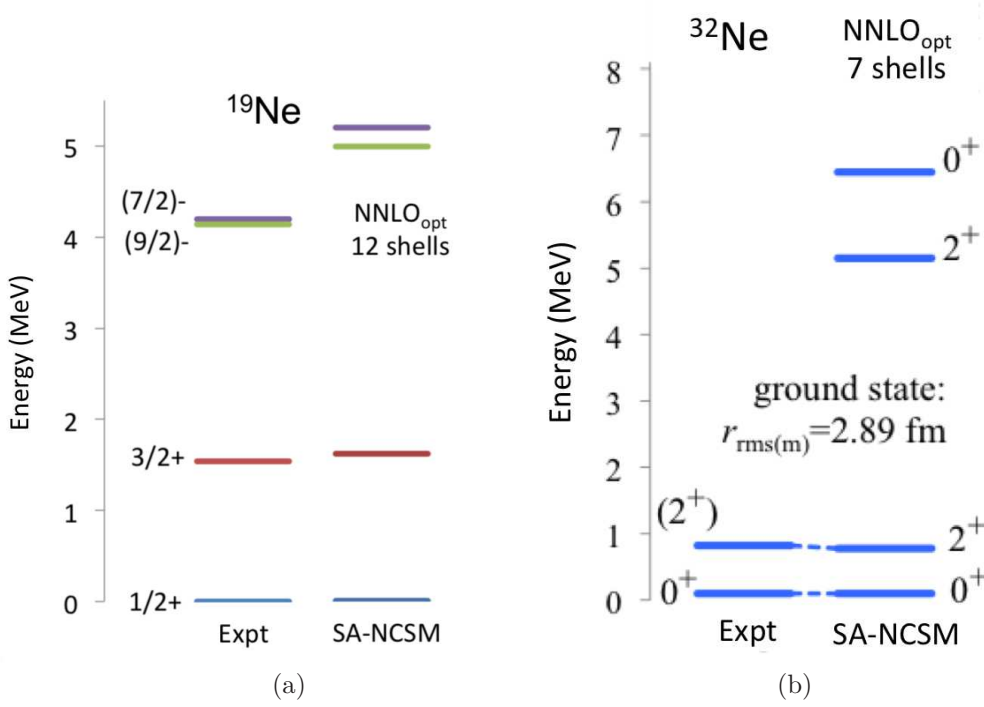


Figure 3: *Ab initio* SA-NCSM calculations using the chiral NNLO_{opt} NN interaction [31] for excitation spectra in (a) ^{19}Ne with 12 HO major shells and (b) ^{32}Ne with 7 HO major shells. Simulations are performed on the Blue Waters system.

^{32}Ne in 7 HO major shells [29]). Further, medium mass nuclei (e. g., ^{48}Ti in 8 HO major shells [29]) are now within the reach of the SA-NCSM. All of these results utilize realistic chiral interactions and were able to incorporate contributions from higher HO major shells than previously achievable in order to allow the development of the most important configurations in each nucleus. The results show good agreement with experiment, especially as related to collectivity, a traditionally challenging feature for *ab initio* models to reproduce. For example, the quadrupole moment for the first 2^+ state in ^{48}Ti from experiment is known to be $-17.7 e \cdot \text{fm}^2$ [30] and SA-NCSM calculations show a value of $-19.3 e \cdot \text{fm}^2$ based on the chiral NNLO_{opt} NN interaction [31] in 8 HO major shells with no effective charges. This indicates that the symmetry-adapted basis is capable of allowing the necessary collectivity to develop while also controlling the combinatorial growth associated with standard NCSM model spaces.

To further study the collectivity, especially with respect to the isospin symmetry breaking effects in mirror nuclei, we carry forward a systematic study of $B(E2)$ values in mirror nuclei. Traditionally the isospin symmetry breaking has been studied by comparing the level energies in mirror nuclei or their masses. To advance the understanding of isospin symmetry breaking effects, a range of spectroscopic data is required, including the $B(E2)$ values, in addition to the energies of excited states. For example, Fig. 4 shows *ab initio* SA-NCSM calculation results for ^{21}Mg and ^{21}F mirror nuclei. Calculations of $B(E2)$ strengths were performed using various symmetry-based selections of the SA-NCSM model space and $\hbar\Omega$ values, and only the results with

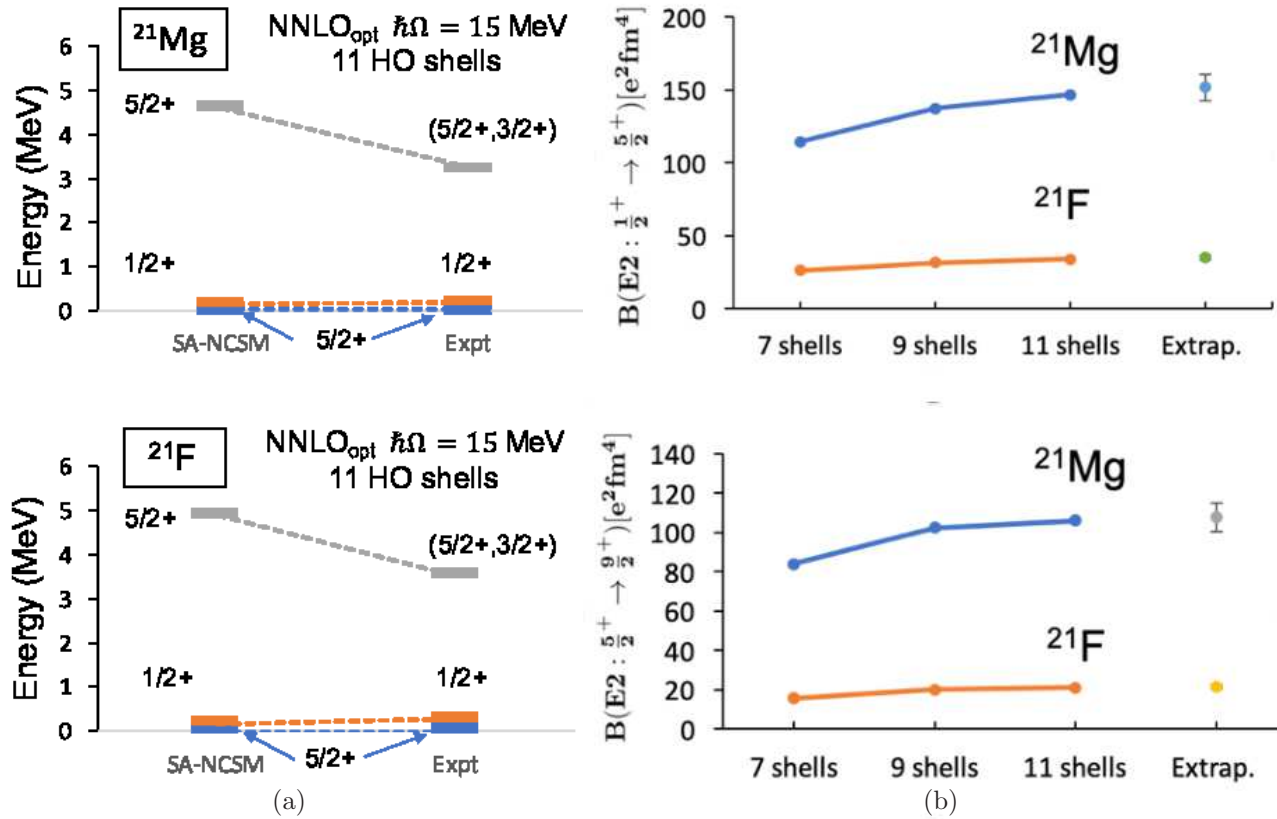


Figure 4: *Ab initio* SA-NCSM calculations using the chiral NNLO_{opt} NN interaction [31] in ultra-large model spaces ($\hbar\Omega = 15$ MeV). (a) Energy spectrum of ^{21}Mg and ^{21}F in 11 HO major shells, and (b) convergence of the $B(E2 : \frac{1}{2}^+ \rightarrow \frac{5}{2}^+)$ (top) and $B(E2 : \frac{5}{2}^+ \rightarrow \frac{9}{2}^+)$ (bottom) strengths with increasing model space, and the extrapolated values with uncertainties from model space and $\hbar\Omega$ variance. Simulations are performed on the Blue Waters system. Experimental values for the $B(E2)$ are available in Ref. [32].

the most optimal parameters that show the fastest convergence trend are depicted in Fig. 4. The variance of the model spaces and HO parameter $\hbar\Omega$ is accounted for the extrapolated values and their uncertainties. These results compare to the recent experimental values [32] reasonably well, demonstrating the SA-NCSM capability to describe collectivity in these challenging mirror nuclei.

4 Canonical transformations

The symplectic $\text{Sp}(3, \mathbb{R})$ group is the group of linear canonical transformations in phase space [33]. We use this fact to define a linear unitary canonical transformation that maps the generators of the $\text{sp}(3, \mathbb{R})$ algebra into a deformed equivalent set while preserving the symplectic symmetry. We expect that the associated deformed basis states can capture the dominant physics of deformed systems in smaller model spaces, which, in turn, reduces the computational resource requirements.

In classical mechanics, canonical transformations are a set of transformations that preserve the Poisson brackets between generalized coordinates and momenta,

$$\{q_i, p_j\} = \{\tilde{q}_i, \tilde{p}_j\} = \delta_{ij}. \quad (3)$$

The generalization of this definition to the quantum mechanical case is achieved if one replaces the Poisson brackets with commutation relations between the coordinate and momentum operators.

$$[q_i, p_j] = [\tilde{q}_i, \tilde{p}_j] = i\delta_{ij}. \quad (4)$$

Furthermore, the canonical transformations in classical mechanics are always unitary transformations. However, this is not necessarily the case in quantum mechanics [34]. In quantum mechanics, a canonical transformation can be unitary or non-unitary [35, 36]. For the purpose of constructing a deformed basis, we will limit ourselves to unitary transformations. Now we define the following unitary canonical transformations:

$$\begin{aligned} \tilde{q}_i &= \frac{1}{\sqrt{\epsilon_i}} q_i, \\ \tilde{p}_i &= \sqrt{\epsilon_i} p_i, \end{aligned} \quad (5)$$

where ‘ \sim ’ denotes the quantities in the canonically deformed space, and the ϵ_i ’s are the deformation parameters (real positive quantities) that define the specifics of the transformation. The physical implication of ϵ_i depends on the system being studied. If we choose $\epsilon_i = \omega/\omega_i$ where ω_i is the HO frequency in the i -th direction, then ϵ_i could be interpreted as a deformation parameter that transforms the non-deformed canonical set (q_i, p_i) into the deformed canonical set $(\tilde{q}_i, \tilde{p}_i)$. It is important to note that these canonical transformations not only preserve the Heisenberg algebra, but also preserve the symplectic algebra such that it closes under commutation just as the non-deformed algebra does [37].

Using the canonical transformations defined above, we construct the deformed harmonic oscillator creation and annihilation operators in terms of non-deformed

ones,

$$\begin{aligned}\tilde{b}_{in}^+ &= \frac{1}{2} \left(\frac{1}{\sqrt{\epsilon_i}} (b_{in}^+ + b_{in}) + \sqrt{\epsilon_i} (b_{in}^+ - b_{in}) \right), \\ \tilde{b}_{in} &= \frac{1}{2} \left(\frac{1}{\sqrt{\epsilon_i}} (b_{in}^+ + b_{in}) - \sqrt{\epsilon_i} (b_{in}^+ - b_{in}) \right).\end{aligned}\tag{6}$$

It is easy to see that the canonical transformations in Eqs. (6) are equivalent to Eqs. (5), and therefore

$$[b_{in}, b_{jn}^+] = [\tilde{b}_{in}, \tilde{b}_{jn}^+] = \delta_{ij},\tag{7}$$

which are equivalent to Eq. (4).

The canonical transformations defined in Eqs. (5) are symmetric with respect to inverse transformations. The inverse transformations are achieved if one removes ‘ \sim ’ from the deformed quantities and adds it to the non-deformed quantities and then flips the deformation coefficients. To demonstrate this, we apply this procedure of inverse transformation to Eq. (5) by making the substitution ($\tilde{q}_i \rightarrow q_i, \tilde{p}_i \rightarrow p_i$), then flipping the coefficients $\frac{1}{\sqrt{\epsilon_i}} \rightarrow \sqrt{\epsilon_i}$, $\sqrt{\epsilon_i} \rightarrow \frac{1}{\sqrt{\epsilon_i}}$, and we get

$$\begin{aligned}q_i &= \sqrt{\epsilon_i} \tilde{q}_i, \\ p_i &= \frac{1}{\sqrt{\epsilon_i}} \tilde{p}_i,\end{aligned}\tag{8}$$

which are the inverse transformations.

Using the canonical transformations, we express the many-body HO Hamiltonian in terms of the deformed symplectic operators in $\hbar\omega$ units,

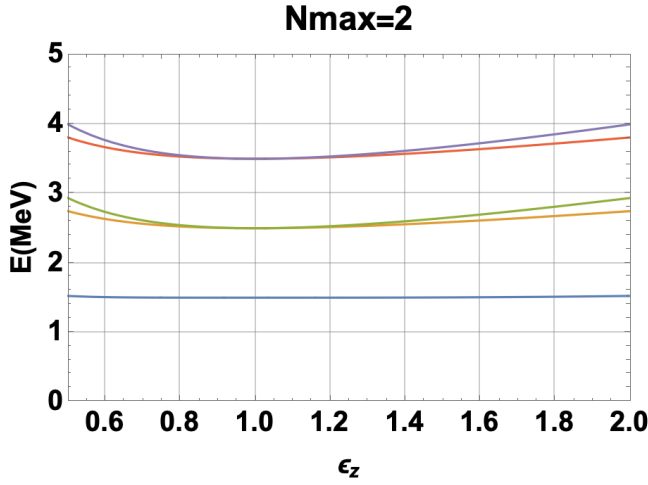
$$H = \sum_i C_{ii} = \frac{1}{4} \left(\epsilon_i (\tilde{A}_{ii} + \tilde{B}_{ii} + 2\tilde{C}_{ii}) + \frac{1}{\epsilon_i} (-\tilde{A}_{ii} - \tilde{B}_{ii} + 2\tilde{C}_{ii}) \right),\tag{9}$$

where, for simplicity, $\epsilon_x = \epsilon_y$ has been chosen with the constraint $\epsilon_x \epsilon_y \epsilon_z = 1$ which implies volume conservation of the system. Then Eq. (9) reduces to

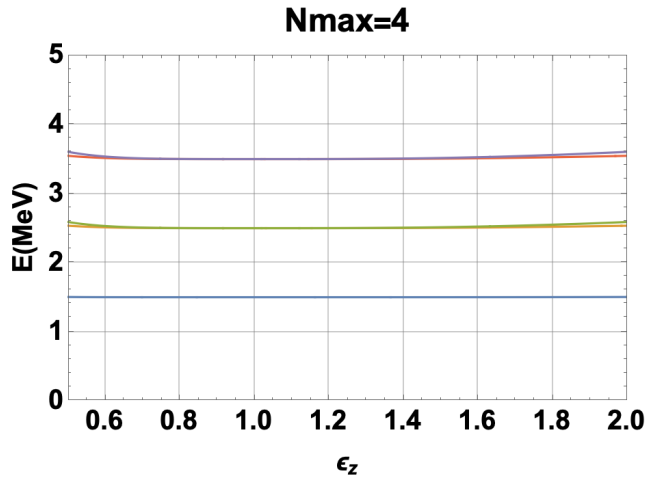
$$H = \frac{1}{4} \left(\left(\epsilon_z - \frac{1}{\epsilon_z} \right) (\tilde{A}_{zz} + \tilde{B}_{zz}) + 2 \left(\sqrt{\epsilon_z} + \frac{1}{\sqrt{\epsilon_z}} \right) (\tilde{C}_{xx} + \tilde{C}_{yy}) + 2 \left(\epsilon_z + \frac{1}{\epsilon_z} \right) \tilde{C}_{zz} \right).\tag{10}$$

Diagonalizing the Hamiltonian in Eq. (10) for a single particle within a model space of $N_{\max} = 2$ and $N_{\max} = 4$ we get results shown in Fig. 5. We expected to see all the eigenvalues independent of ϵ_z , however Fig. 5 shows a slight dependence of the eigenvalues on ϵ_z . This is because we are attempting to map from an infinite Hilbert space onto a finite Hilbert space, which one can only do approximately by going to higher and higher N_{\max} values; that is, the transformation from the non-deformed to deformed set of operators is not truly a unitary one. To get a unitary transformation, that will be independent of ϵ_z , one has to map it onto infinite deformed basis states which is not possible, but as the figures show, with increasing N_{\max} the results seem to converge very nicely to the low-lying eigenvalues by the time $N_{\max} = 4$.

Note that when we applied the canonical transformations to the harmonic oscillator Hamiltonian in Eq. (9), the operator C_{ii} includes the zero point energy or the so-called vacuum energy in its definition. It is usually common practice in quantum mechanics and quantum field theories to renormalize the energy by discarding the



(a)



(b)

Figure 5: The eigenvalues (in $\hbar\omega$ units) of a 3D spherical HO as a function of ϵ_z in the deformed model spaces of $N_{\max}=2$ (a) and $N_{\max}=4$ (b) where $\epsilon_x = \epsilon_y$ and the $\epsilon_x \epsilon_y \epsilon_z = 1$ constraint applies.

vacuum contribution to the energy since it has no physical meaning. However, the vacuum term should be included when applying canonical transformations because it is part of the symplectic algebra $\text{sp}(3, \mathbb{R})$. In order to unitarily map the symplectic operators to their deformed counterparts, one also needs to map the vacuum to its deformed counterpart. After the mapping one could renormalize the energy by throwing away the deformed vacuum. The vacuum term in C_{ii} for a single particle is $\frac{3}{2}$ which, after applying the canonical transformation becomes $6\left(\sqrt{\epsilon_z} + \frac{1}{\sqrt{\epsilon_z}}\right) + 3\left(\epsilon_z + \frac{1}{\epsilon_z}\right)$ for $\epsilon_x = \epsilon_y$ and $\epsilon_x \epsilon_y \epsilon_z = 1$.

5 Conclusions

A short ‘Historical overview’ of multi-shell-model efforts to understand observed features of light nuclei is given in Section 2. The focus is on ‘open-shell’ methods —

commonly called the NCSM, where nucleons are allowed to occupy any and all valence shells of a 3D HO that include excited configurations up to an aggregated N_{\max} value coupled with the use of *ab initio* rather than schematic interactions within that space. These concepts, introduced around the turn of the last century, serves as a demarkation between ‘old’ and ‘new’ in the evolution of the shell-model for reproducing and predicting nuclear phenomena. Our focus within this framework is on the use of symmetries to tame the exponential grow of model spaces, which otherwise await the availability of ever larger and faster high-performance computing resources and/or various extrapolation procedures for further advances within this NCSM framework.

Section 3 gives some examples of how one can beat back the exponential growth of NSCM spaces through the recognition and use of special symmetries that track with dominant modes in nuclei. A dominant feature that stands above all others is strong $B(E2)$ transition strengths between members of rotational bands. This feature, which is correlated with the emergence of coherent states that organizes the NSCM landscape into various shapes, which was foreshadowed by early successes of collective models like that of Bohr and Mottelson [8] as well as that of Nilsson [38] and the so-called Geometrical Collective Model of Greiner and associates [9, 10], which extend to odd- A nuclei with an uncoupled nucleon residing within the collective geometrical shape defined by that of the others. This collusion among nucleons that leads to collective configurations, which can be characterized as a co-existence of geometrical shapes, tracks with Elliott’s SU(3) Model [11, 12] within a single shell and its multi-shell extension, the symplectic shell model, Sp(3, \mathbb{R}) [19] that in its most rudimentary form can be envisioned as the addition HO quanta (via particle excitations) of the monopole and quadrupole type to the simplest of $N_{\max} = 0$ configurations.

What this picture suggests, as it did in the earliest days via the Nilsson Model [38], is moving to a deformed geometry from the onset might define a smarter path forward. In Section 4 we show results which suggest that this can be achieved while simultaneously maintaining all the advantages of the symplectic shell-model picture through exploitation of a canonical transformation away from spherical symmetry to a deformed geometry that preserves commutation relations of the symplectic algebra while maintaining the unitarity of the transformation. From a practical perspective this means that everything learned and developed for a spherical symplectic picture can be brought forward into a deformed symplectic picture. As suggested above, this can be seen as an interacting many-particle generalization of the Nilsson Model. While additional work remains to be done, the underlying feature of this evolving picture look promising for its overarching simplicity; namely, the accommodation of what requires high N_{\max} values within a spherical geometry within lower \tilde{N}_{\max} model spaces of a deformed geometry. It also suggests that the development and application of a deformed symmetry-adapted NCSM for nuclei may soon be within reach.

Acknowledgements

Support from the U.S. National Science Foundation (OIA-1738287 and ACI-1713690) and the U.S. Department of Energy (DE-SC0005248), as well as those from Louisiana State University, especially computational resources under the Louisiana Optical Network Initiative, and the Southeastern Universities Research Association are all gratefully acknowledged.

References

- [1] M. G. Mayer, Phys. Rev. C **75**, 1969 (1949).
- [2] O. Haxel, J. H. D. Jensen and H. E. Suess, Phys. Rev. **75**, 1766 (1949).
- [3] P. Navrátil, J. P. Vary and B. R. Barrett, Phys. Rev. Lett. **84**, 5728 (2000).
- [4] B. Barrett, P. Navrátil and J. Vary, Prog. Part. Nucl. Phys. **69**, 131 (2013).
- [5] P. Navrátil, S. Quaglioni, I. Stetcu and B. R. Barrett, J. Phys. G **36**, 083101 (2009).
- [6] R. Roth and P. Navrátil, Phys. Rev. Lett. **99**, 092501 (2007).
- [7] T. Abe, P. Maris, T. Otsuka, N. Shimizu, Y. Utsuno and J. Vary, Phys. Rev. C **86**, 054301 (2012).
- [8] A. Bohr and B. R. Mottelson, *Nuclear structure*. Benjamin, New York, 1969.
- [9] G. Gneuss, U. Mosel and W. Greiner, Phys. Lett. B **30**, 397 (1969).
- [10] J. Eisenberg and W. Greiner, *Nuclear theory I: Nuclear collective models*. North-Holland, Amsterdam, 1987.
- [11] J. P. Elliott, Proc. Roy. Soc. A **245**, 128 (1958).
- [12] J. P. Elliott and M. Harvey, Proc. Roy. Soc. A **272**, 557 (1962).
- [13] C. Bahri, J. Draayer and S. Moszkowski, Phys. Rev. Lett. **68**, 2133 (1992).
- [14] A. Zuker, J. Retamosa, A. Poves and E. Caurier, Phys. Rev. C **52**, R1741 (1995).
- [15] G. Rosensteel and D. J. Rowe, Phys. Rev. Lett. **38**, 10 (1977).
- [16] D. J. Rowe, Rep. Prog. Phys. **48**, 1419 (1985).
- [17] K. D. Launey, T. Dytrych and J. P. Draayer, Prog. Part. Nucl. Phys. **89**, 101 (2016).
- [18] D. Rowe, AIP Conf. Proc. **1541**, 104 (2013).
- [19] A. C. Dreyfuss, K. D. Launey, T. Dytrych, J. P. Draayer and C. Bahri, Phys. Lett. B **727**, 511 (2013).
- [20] T. Dytrych, K. D. Sviratcheva, J. P. Draayer, C. Bahri and J. P. Vary, J. Phys. G **35**, 123101 (2008).
- [21] K. D. Launey, A. C. Dreyfuss, J. P. Draayer, T. Dytrych and R. B. Baker, J. Phys. Conf. Ser., **569**, 012061 (2014).
- [22] D. J. Rowe, Phys. Rev. **162**, 866 (1967).
- [23] D. J. Rowe, G. Thiamova and J. L. Wood, Phys. Rev. Lett. **97**, 202501 (2006).

- [24] A. C. Dreyfuss, J. P. Draayer, K. D. Launey, T. Dytrych and R. B. Baker, in *Proc. 6th Int. Conf. on Fission and Properties of Neutron-Rich Nucl. — ICFN6, November 6–12, 2016, Sanibel Island, Florida, USA*, eds. J. H. Hamilton, A. V. Ramayya and P. Talou. World Scientific, Singapore, 2017.
- [25] A. C. Dreyfuss, K. D. Launey, T. Dytrych, J. P. Draayer, R. B. Baker, C. M. Deibel and C. Bahri, *Phys. Rev. C* **95** (2017).
- [26] K. D. Launey, T. Dytrych, J. P. Draayer, G. K. Tobin, M. C. Ferriss, D. Langr, A. C. Dreyfuss, P. Maris, J. P. Vary and C. Bahri, in *Proc. 5th Int. Conf. on Fission and Properties of Neutron-Rich Nucl. — ICFN5, November 4–10, 2012, Sanibel Island, Florida, USA*, eds. J. H. Hamilton and A. V. Ramayya. World Scientific, Singapore, 2013.
- [27] G. K. Tobin, M. C. Ferriss, K. D. Launey, T. Dytrych, J. P. Draayer and C. Bahri, *Phys. Rev. C* **89**, 034312 (2014).
- [28] J. P. Draayer, K. D. Launey, T. Dytrych, A. C. Dreyfuss, G. H. Sargsyan and R. B. Baker, in *Walter Greiner memorial volume*, eds. P. O. Hess and H. Stöcker. World Scientific, Singapore, 2018, p. 97.
- [29] K. D. Launey, A. Mercenne, G. H. Sargsyan, H. Shows, R. B. Baker, M. E. Miora, T. Dytrych and J. P. Draayer, *AIP Conf. Proc.* **2038**, 020004 (2018).
- [30] J. W. Lightbody, Jr., *Phys. Lett. B* **38**, 475 (1972).
- [31] A. Ekström, G. Baardsen, C. Forssén, G. Hagen, M. Hjorth-Jensen, G. R. Jansen, R. Machleidt, W. Nazarewicz, T. Papenbrock, J. Sarich and S. M. Wild, *Phys. Rev. Lett.* **110**, 192502 (2013).
- [32] P. Ruotsalainen *et al.*, *Phys. Rev. C* **99**, 051301(R) (2019).
- [33] M. Moshinsky and C. Quesne, *J. Math. Phys.* **12**, 1772 (1971).
- [34] A. Anderson, *Ann. Phys. (NY)* **232**, 292 (1994).
- [35] P. A. Mello and M. Moshinsky, *J. Math. Phys.* **16**, 2017 (1975).
- [36] J. Deenen, M. Moshinsky and T. Seligman, *Ann. Phys. (NY)* **127**, 458 (1980).
- [37] J. P. Draayer, *Retrospective Theses and Dissertations* 3731 (1968).
- [38] S. G. Nilsson, *Dan. Mat. Fys. Medd.* **29**, 16 (1955).